Renewable Energy 133 (2019) 787–796

Contents lists available at ScienceDirect

Renewable Energy

journal homepage: www.elsevier.com/locate/renene

PV system design with the effect of soiling on the optimum tilt angle

Ricardo Conceição [a, b, *], Hugo G. Silva [a, b], Luis Fialho [a], Francis M. Lopes [a], Manuel Collares-Pereira [a, b]

[a] Renewable Energies Chair, University of Évora, Portugal
[b] Instituto Ciências da Terra, Universidade de Évora, Portugal

ARTICLE INFO

Article history:
Received 29 January 2018
Received in revised form
17 September 2018
Accepted 17 October 2018
Available online 22 October 2018

Keywords:
solar energy
PV performance
Soiling
Optimum tilt angle

ABSTRACT

Local particle deposition and solar irradiance data, from Photovoltaic Geographical Information System (PVGIS) in the Alentejo region (southern Portugal), are used for the development of a modified effective irradiance model featuring soiling. The model allows to calculate the optimum tilt angle for soiled PV systems, as the inclusion of soiling gives realistic results for different tilt angles to be used in the absence of cleaning; instead of using an optimum tilt angle solely based on irradiance. Consequently, the proposed model enables an increase of maximum energy production and the design of multiple tilt angle configurations to further maximize the annual energy yield, regarding a common fixed structure. The presented calculations include the seasonal soiling effect for the region, showing the applicability that this type of approach has for multiple tilt angle configurations. An economic analysis is also carried out to choose the best design, taking into account the trade-off between the increase in energy production and the costs of changing the tilt angle. The effective irradiance model for clean and soiled scenarios is also explored with the development of a method to infer when a PV installation should be cleaned for the desired efficiency.

1. Introduction

Among all factors that can influence Solar Energy Plants (SEP) operations [1], the accumulation of dirt (e.g. dust, pollen and bird dropping) on top of Solar Energy Systems (SES) surfaces; namely on photovoltaic (PV) glass, has been receiving more attention recently. This accumulation is known as soiling and is considered to be the third most important environmental factor influencing SES performance [2]. Soiling reduces the effective irradiance absorption by PV cells and, consequently, significant power losses take place [3], leading to a decreasing of power generation as much as 50% in extreme climates, such as deserts [4]. In southern Portugal, a decrease of ≈ 8% has been observed [5], showing how soiling can significantly influence SEP operations, even in non-desert regions, and with worse effects in concentrated solar power technologies [6].

Adding soiling to the cell-temperature effect, will determine a significant performance decrease from the expected nominal performance. One approach to reduce soiling effect is the use of anti-soiling coatings [2], however these still need to be further researched. Thus, the available and reliable way to handle soiling nowadays, is to regularly clean the affected surfaces, especially in regions where the number of particles in the atmosphere is exceptionally high, causing considerable reduction of system performance. Currently, the only viable cleaning option for PV panels (or glass surfaces in general) is through manual cleaning or automated robots. If solar plants are economically able to afford expensive robotic solutions, then soiling becomes a minor problem. However, for PV plants that are not able to support the cost of such technology or for smaller plants and private owners without an easy access to the PV system (e.g. roof installation), designing the system to take into account the local soiling would be significantly valuable. This would reduce cleaning tasks and would also increase energy production.

The first objective of the present work is to study the optimum tilt angle considering soiling, focusing in the maximization of energy production, taking into account the soiling effect in the absence of cleaning schedules, as this is still not a widely studied subject. To develop such model, several aspects are considered. Firstly, measured data is required as an input variable for the in-situ model, particularly solar irradiance measured at ground-level (if available, it should be used instead of satellite data). Secondly, dust

* Corresponding author. Renewable Energies Chair, University of Évora, Portugal.
E-mail address: rfc@uevora.pt (R. Conceição).

https://doi.org/10.1016/j.renene.2018.10.080
0960-1481/

deposition should be considered as function of the tilt angle, which is also a local feature [7]; for instance, dew, turbulence, wind speed and direction, can modify the amount of particle deposition [8]. Thirdly, it is necessary to have transmittance measurements of the PV glass covered with soiling accumulated on site, since the same number of different types of particles can lead to different transmittance losses [9]. These models are then introduced in a general model of irradiance considering soiling, enabling an estimation of their effects on PV plants.

Another objective of this work is to calculate multiple soiled tilt angle configurations throughout the year, which can be deployed using movable frames, and can range from 2 to 12 tilt angles per year, simultaneously studying the soiling effect on the energy production of these configurations compared to a fixed structure. Moreover, it is presented a method considering the comparison between dirty and clean scenarios, allowing the PV system owner to determine the best periodicity to perform scheduled cleaning.

This topic has still not been fully developed and for that matter literature concerning advances in the effects of soiling in PV systems is still scarce [10,11]. The approach used in Ref. [10] is based on the dependency of soiling with the tilt angle. However, in such study, the particle deposition is assumed to be constant for all months, which is an unrealistic scenario, due to the season variability of precipitation and other environmental conditions. The present work explores soiling on a monthly basis, since soiling variability is one of the most important aspects of particle deposition. Furthermore, multiple tilt angle configurations are explored in order to include the annual irradiance and soiling variability, as well as, an economic analysis to determine the optimum configuration. It should be mentioned that the approach used by Lu and Hajimirza [11] has valuable meaning, since it is based on panel length and friction coefficients. However, such analysis is different from the one presented here, since it is performed with respect to the solar zenith angle, which implies a 2-axis tracking. Similarly, the work carried out by Xu and co-workers [10], does not include a multiple tilt angle analysis, a resulting economic analysis and does not explore the development of cleaning schedules, as shown here.

The present work aims to demonstrate how soiling can be mitigated by changing the tilt angle of the PV modules, for both constant and multiple tilt angles throughout the year. Moreover, for multiple annual configurations, it is necessary to take into account the annual variation of particle deposition and irradiance and, for that matter, an economic analysis is performed to maximize profitability. Finally, a different use for the approach developed in this work is presented: the derivation of cleaning schedules, for any given loss of system performance efficiency degradation.

The remainder of this paper is structured as follows: Section 2 explains how the irradiance and soiling were processed and modelled; Section 3 presents an analysis of optimum tilt angles from a fixed to a 12-tilt angle configuration, to determine the best potential configuration relatively to the fixed one; Section 4 uses the model to determine the PV panels cleaning schedule, defining the yearly cleaning period when losses surpass a certain threshold; final conclusions and remarks are summarized in Section 5.

2. Irradiance and soiling modelling

2.1. Irradiance modelling

This subsection describes how irradiance on a tilted plane, β, is modelled. The total irradiance on a tilted surface, I_{coll}, is composed of direct, $I_{bn}\cos(\theta)$, sky-diffuse, $I_d\left(\frac{1+\cos\beta}{2}\right)$, and ground reflected components, $I_h\rho_g\left(\frac{1-\cos\beta}{2}\right)$, as depicted in Fig. 1. It should be noted

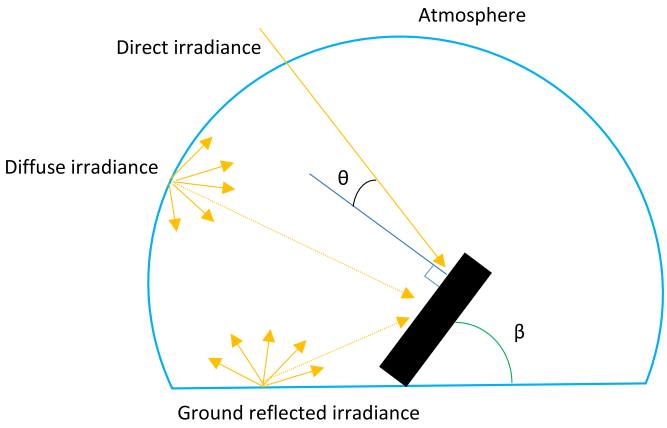

Fig. 1. Irradiance components scheme.

that I_{bn}, I_d and I_h represent the beam, diffuse and global horizontal irradiance, respectively.

The total irradiance can be mathematically described [12] as shown in Eq. (1):

$$I_{coll} = I_{bn}\cos(\theta) + I_d\left(\frac{1+\cos\beta}{2}\right) + I_h\rho_g\left(\frac{1-\cos\beta}{2}\right), \quad (1)$$

where $\cos(\theta)$ is the angle between the beam irradiance and the surface normal, while ρ_g is the ground albedo coefficient. The direct irradiance component is obtained using simple geometry, while the diffuse component is determined with the Liu-Jordan isotropic model [13,14] and the albedo component through the classic isotropic approach. The variable $\cos(\theta)$ can be calculated straightforward, using spherical geometry, as given by Eq. (2):

$$\cos\theta = \cos(\delta)\cos(\phi-\beta)\cos(\omega) + \sin(\delta)\sin(\phi-\beta), \quad (2)$$

where δ, ϕ and ω are the declination, latitude and hour angle, respectively. Regarding the ground reflected irradiance, there is a lack of a robust database for ρ_g, since in-situ measurements are non-existing. However, the typical approach to overcome this is to consider $\rho_g = 0.2$ [12], and thus, calculations concerning the ground reflected irradiance were performed using this value as reference.

Solar irradiance data was taken from PVGIS [15], despite the fact that local data is available for all of the above irradiance components, except for albedo, to highlight the general application of the method. Typical meteorological days were used in the analysis.

2.2. Effective irradiance model with soiling

For the effective irradiance that reaches the PV panels on a given tilt angle β, the model described in Ref. [16] is used, as shown by Eq. (3):

$$G_{eff} = \tau_r\left[(1-L_b)I_{bn}\cos(\theta) + (1-L_d)I_d\left(\frac{1+\cos\beta}{2}\right) + (1-L_a)I_h\rho_g\left(\frac{1-\cos\beta}{2}\right)\right], \quad (3)$$

where τ_r is the normal incidence transmittance ratio for soiled and clean glass PV cover, while L_b, L_d and L_a are angular loss factors for direct, diffuse and albedo components, respectively. The variable τ_r is calculated through Eq. (4), as follows:

$$\tau_r = \frac{\tau_{soiled}}{\tau_{clean}}, \quad (4)$$

while angular loss factors from Ref. [16] are calculated as follows, in Eqs. (5)–(7):

$$L_b = \frac{\exp\left(-\frac{\cos\theta}{a_r}\right) - \exp\left(-\frac{1}{a_r}\right)}{1 - \exp\left(-\frac{1}{a_r}\right)}, \quad (5)$$

$$L_d = \exp\left[\frac{-c_1}{a_r}\left(\sin\beta + \frac{\pi - \beta - \sin\beta}{1 + \cos\beta}\right) - \frac{c_2}{a_r}\left(\sin\beta + \frac{\pi - \beta - \sin\beta}{1 + \cos\beta}\right)^2\right], \quad (6)$$

$$L_a = \exp\left[\frac{-c_1}{a_r}\left(\sin\beta + \frac{\beta - \sin\beta}{1 - \cos\beta}\right) - \frac{c_2}{a_r}\left(\sin\beta + \frac{\beta - \sin\beta}{1 - \cos\beta}\right)^2\right], \quad (7)$$

where c_1 and c_2 are the coefficients obtained from a least square fit and a_r is the angular loss coefficient. The angular loss factor for the direct irradiance component corresponds to the ratio between transmittance with a certain incidence angle and transmittance with normal incidence. Both diffuse and albedo angular loss factors are calculated solving two integrals that consider the contribution of each solid angle unit incident on the PV module (assuming an isotropic distribution of diffuse and albedo components).

2.3. Mass accumulation as function of the tilt angle

To account for the effect of soiling on the tilt angle, it is necessary to infer the dependency of mass accumulation with the tilt angle itself. The data needed to model such dependency was obtained using glass samples ($11 \times 9\ cm^2$) in an outdoor environment, mounted on a structure designed and installed in the facilities of the Renewable Energies Chair (REC), University of Évora, designated *Plataforma de Ensaio de Concentradores Solares* (PECS), which is located in southern Portugal (southwest of Europe), 38.5731° N, 7.9044° W, as shown in Fig. 2. This glass tree is able to provide several tilt angle configurations, ranging from 0° to 90° at 15° steps. There are 6 glasses per cardinal direction and one completely horizontal at the top of the structure. In this analysis, only the south glasses were taken into account, since that is the typical azimuth of installed PV systems.

Mass accumulation measurements were performed with a micro-balance (Bosch SAE 80/200). The weight of each glass sample was measured at the end of every week, while the respective monthly means were calculated thereafter. Assuming exponential mass functions of the type $M_A(\beta) = p_1 \exp(p_2\beta)$, monthly dependencies on the tilt angle, $M_A(\beta)$, were then calculated, see Table 1. Due to missing periods of data during the months of December and January, the corresponding $M_A(\beta)$ functions were set equally to the value found for November, as it was found to be the month with less soiling (February is not considered in this assumption since there was a severe and unusual Saharan desert dust event). Additionally, November is a month within the rainy season and, therefore, a reduction in the amount of soiling is expected to occur.

Mass accumulation functions can be seen in Fig. 3, with spring and summer months showing higher soiling, as expected, mainly due to the lack of precipitation. In particular, during April, the highest soiling occurs due to the increase in organic soiling, namely pollen deposition [17]. As shown in Fig. 3, the soiling effect with the tilt angle is approximately exponential in all cases, although the data was smoothed to eliminate bird dropping effects on mass accumulation. The statistical values obtained are summarized in Table 1, where all values of r^2 are above 0.9 (with the majority of them above 0.95) and a RMSE consistently below 0.02, corresponding to reliable approximations.

Fig. 2. Glass tree sampling structure at PECS (southern Portugal).

2.4. Transmittance ratio as function of the tilt angle

In order to model the relation of transmittance ratio with the tilt angle, mass accumulation data was related to the transmittance ratio between dirty and clean glasses. This leads to a linear least square fit that can be obtained through Eq. (8):

$$\tau_r(M_A) = b_1 M_A + 1, \quad (8)$$

where $b_1 = -0.2545\ m^2/g$. Previous studies, for instance [7], have used an exponential model instead of a linear one. However, no high transmittance loss regimes, such as those in desert regions, are present in this data set, justifying the use of a linear fit. Since this is the case for typical urban and rural environments in Europe, the focus of the present work is given to a linear model instead of an exponential one (see Fig. 4), where high correlations (r^2) can be obtained.

With both $\tau_r(M_A)$ and $M_A(\beta)$, it is possible to estimate the transmittance ratio as a function of β and $\tau_r(\beta)$ from Eq. (8), for each month, as follows:

$$\tau_r(\beta) = b_1[p_1 \exp(p_2\beta)] + 1 = b_1 p_1 \exp(p_2\beta) + 1 \quad (9)$$

Table 1
Monthly mean mass accumulation statistics (data retrieved in 2017 at PECS).

Months										
	F	M	A	M	J	J	A	S	O	N
r^2	0.97	0.21	0.95	0.98	0.90	0.91	0.994	0.995	0.99	0.91
RMSE	0.01	0.02	0.18	0.01	0.01	0.03	0.02	0.01	0.02	0.02

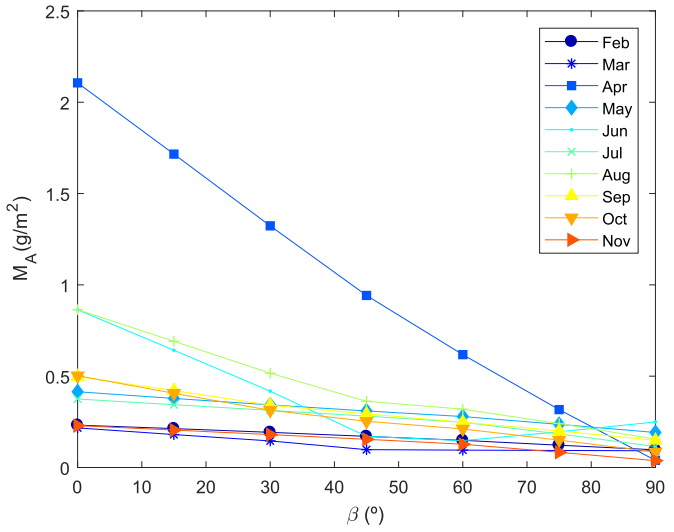

Fig. 3. Mass accumulation as function of the tilt angle for each month (data retrieved in 2017 at PECS).

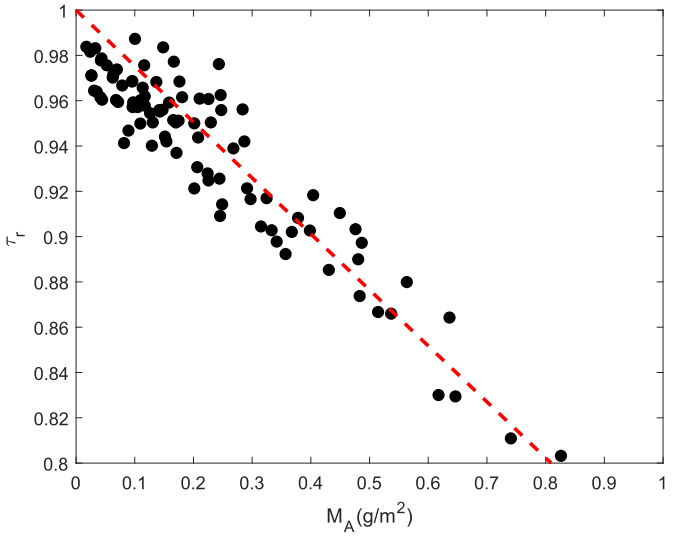

Fig. 4. Transmittance ratio as function of mass accumulation (weight data retrieved in 2017 at PECS and transmittance data retrieved at the Water Laboratory, University of Évora).

2.5. Angular loss coefficients

The angular loss coefficient, a_r, in Eqs. (5)–(7), has a dependency on the transmittance ratio, $a_r(\tau_r)$. Such relation is assumed to be linear and can be obtained through Eq. (10), with data fitting as in Ref. [18]:

$$a_r(\tau_r) = d_1 \Delta\tau + d_2, \tag{10}$$

where $d_1 = -1.23$ and $d_2 = 1.403$, with a r^2 of 0.997. Taking into account that in the present model τ_r is dependent on β, it implies that:

$$a_r(\beta) = a_r[\tau_r(\beta)], \tag{11}$$

thus, alternatively to Eq. (10), a_r can be represented simply by its β dependency:

$$a_r(\beta) = d_1[b_1 p_1 \exp(p_2\beta) + 1] + d_2. \tag{12}$$

The coefficient c_2 is also dependent on the a_r, as described in Ref. [16], therefore a similar process was used, as shown in Eq. (13):

$$c_2(a_r) = f_1 a_r + f_2, \tag{13}$$

where $f_1 = 0.5$ and $f_2 = -0.154$, with a r^2 of 0.99, and, as in a_r, its β dependency can be presented as:

$$c_2(\beta) = f_1 d_1[b_1 p_1 \exp(p_2\beta) + 1] + d_2 + f_2 \tag{14}$$

2.6. Algorithm flowchart

Consequently, for the analysis previously described, all variables depend only on β, on a monthly basis, which allows for Eq. (6) to be calculated considering the angle of incidence, θ, and the tilt angle, β. For a clearer description of the process, a flowchart is presented below (see Fig. 5).

The algorithm presents two processes running in parallel: the calculation of the tilted plane irradiance, I_{coll}, (considered here as the process on the left side) and the soiling implementation (considered here as the process on the right side). With the effective irradiance, G_{eff}, being calculated for each month through Eq. (3) and the effective energy, E_{eff}, obtained by multiplying G_{eff} with the number of days of the respective month, the effective energy can then be calculated for different periods and tilt angles. For instance, if a bi-annual tilt angle configuration is preferred, then every combination of two periods within a year is calculated for every tilt angle (with 1° steps) and then, the respective periods that maximize the annual energy production are chosen.

3. PV design including soiling effect

3.1. Constant tilt angle configuration

As previously explained, the objective of this work is not only to calculate the effective irradiance on the PV plane with soiling, but also to help the design of improved static and quasi-static systems including a realistic soiling model. The static case is useful, for instance, for small PV producers, small domestic rooftop PV systems, small PV plants or Building Integrated Photovoltaics (BIPV), which may be in locations of difficult access. Such situations demand a system designed to include the soiling effect, as it will be discussed in detail, further below.

For a constant optimum tilt angle configuration, which is the

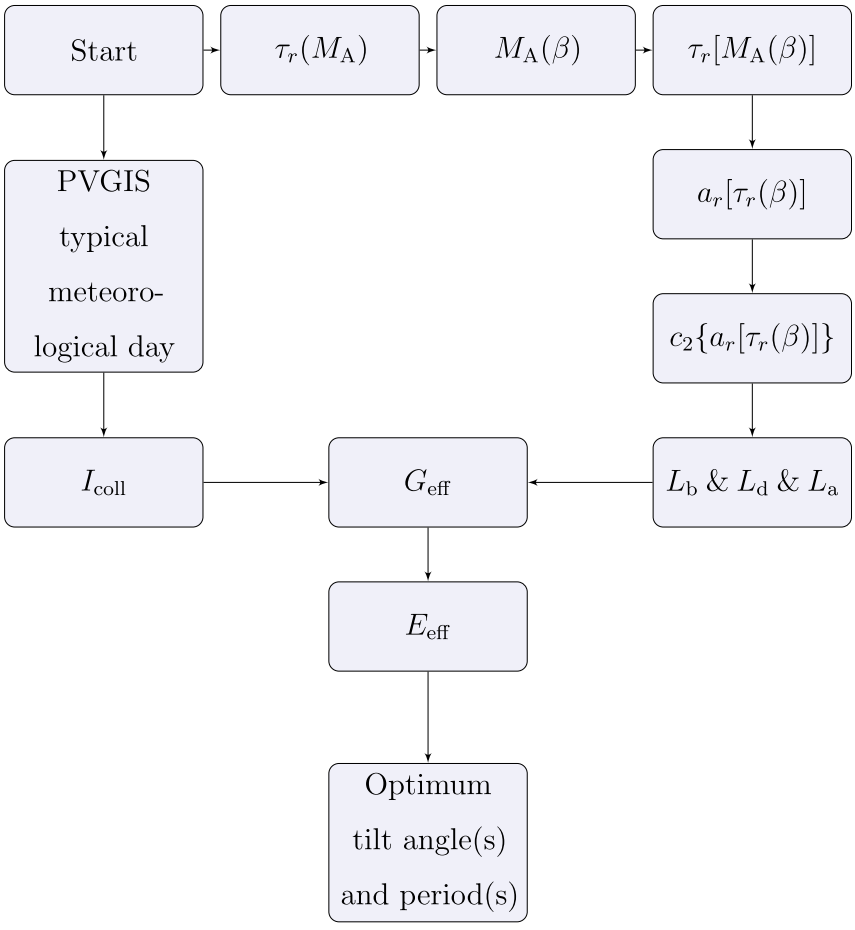

Fig. 5. Algorithm flow chart. Two processes are considered: calculation of the irradiance on the tilted plane (left side) and the soiling implementation (right side). The effective irradiance, G_{eff}, and the effective energy, E_{eff}, are then calculated.

most common setup due to higher maintenance and operational costs associated with tradititonal tracking systems, there is a shift of 6° in the tilt angle. This value is substantially higher when compared with other estimations [10]. In Table 2, for comparison purposes, it is depicted the tilt angle shift, in magnitude, obtained in Ref. [10] and in this work, for a constant tilt angle. It should be noted that the values obtained in Ref. [11] are dependent on the solar zenith, which can direct the according analysis to a full and not manual tracking, as studied here, and for that reason it is not considered in the present analysis.

This analysis may be helpful for small PV installations, where it can be difficult to perform cleaning task. Such technique allows the modules to be tilted considering soiling effects *a priori*, reducing cleaning needs, while maximizing the energy production. It should be noted that the optimum tilt angle for the clean model is 34° on the test site coordinates, which is identical to the one obtained with PVGIS for the same location. This highlights a high correlation between the present model and the PVGIS algorithm for the optimum angle results. From a clean to a soiled scenario, the optimum tilt angle shift, showing that not only depends on local soiling, but on irradiance, as well. The trade-off between these two variables is what dictates such shift.

Table 2
Comparison between tilt angle shift (in magnitude) between present work and [10], for a constant tilt angle in a soiled scenario.

	Present work	Xu and co-workers
Tilt angle shift (°)	6	0.17

3.2. Multiple tilt angle configurations

The previous analysis is relevant for static systems, which are currently the most common. This work also intends to show how quasi-static systems, considering a set of different tilt angles throughout the year, can have their design enhanced considering soiling effect and therefore allowing a power production maximization. In Table 3, in the appendix section, results from 1 to 12 tilt angles per year, with and without soiling, are shown. It is also observed that increasing the system flexibility with respect to the tilt, more energy can be produced, as expected. Values of R_{SS}, i.e. the percentage ratio between the annual effective energy of a specific configuration and the constant tilt one, ranges from ≈ 3.2% for a bi-annual tilt configuration to ≈ 4.3% for a 12 tilt angle configuration. Another conclusion is that periods for soiled scenarios may be different from the clean ones. Therefore, an optimum tilt angle for scenarios with soiling is different in value and also has different operation periods for each tilt angle. Interestingly, above 5 annual tilt angles, no significant increase in the effective energy is observed. This will be further discussed in detail.

The results for the clean scenario, in Table 3, show that the optimum tilt angle for a multiple tilt configuration throughout the year is higher in winter-autumn and lower in spring-summer, as expected, due to the sun's elevation. However, if soiling is considered, the optimum tilt angle changes, as well, the operating periods for each tilt angle (compared to the constant angle setup). It should

be noted that, due to higher soiling levels in April and June, the soiled model increases the tilt angle relatively to the clean model, in order to maximize energy production during these periods. To increase the reliability of the soiled model predictions, additional years of soiling data are needed. Soiling and irradiance have inter-annual variations and can change significantly from site to site. Consequently, it is also recommended the use of several years of soiling data.

In Fig. 6, the effective energy as function of β, with and without soiling for every month, is depicted. Results show a shift on the optimum tilt angle from lower to higher values regarding the clean and soiled scenarios. This transition is related to the fact that soiling is higher at lower tilt angles, causing the increase of the optimum tilt angle in order to reduce the soiling effect.

3.2.1. Trade-off between produced energy and configuration

To maximize energy production, it is important to determine the best system configuration; for that matter, some effort is required to change the PV system tilt angle, increasing maintenance and operation costs (*OPEX*). The system can be installed with movable frames for easier tilt changes (commercially existing nowadays), for instance the one in Fig. 7, from UNISTRUT Service Company (www.unistrutusa.com):

These systems are not automatic, however they are less expensive and do not require maintenance, being therefore easy to install and use. Such systems constitute an option providing an optional and practical way to implement the methods discussed in this work.

In order to choose the best configuration, the *CAPEX* and *OPEX* of a 1 MWp plant with constant tilt was considered. The respective data was gathered from the 2017 European Photovoltaic Technology and Innovation Platform, [19]. A 25-year period analysis was then performed, which is a common period for the operation of PV plants. Considering a fixed frame, the *CAPEX* was taken to be $\approx$ 800 €/kWp and *OPEX* $\approx$ 15 €/kWp. The *CAPEX* and *OPEX* for any of the other configurations, with movable frames, are set as a percentage increase of their values for a fixed structure. The variables *CP* and *OP* represent the percentage increase of *CAPEX* and *OPEX*, respectively. It should be noted that $N_T OP$ represents the number of times that the tilt angle is changed. The energy price, represented by the variable kWh_p, was retrieved from OMIE's website (www.omel.es) and was set as 5.5 c€/kWh, while an average performance ratio, *PR*, of 0.82 was considered for this region (above the 0.8 commonly used), since soiling effect is already present in the annual effective energy calculated. It is assumed that annual PV specific yield, *SY*, in kWh/kWp, is equal to the annual effective energy. Multiplying the performance ratio by the specific yield as the income and taking the *CAPEX* and *OPEX* to represent full cost, a profitability index, *PI*, was created to evaluate the difference between all configurations with respect to the fixed one (see Eq. (15)). It should be noted that, these calculations are performed for a 25-year period with a *CAPEX* and *OPEX* variation for every multiple tilt angle configuration.

$$PI = A_{\text{conf}} - B_{\text{fixed}}, \tag{15}$$

where:

$$A_{\text{conf}} = \sum_{j=1}^{25} SYkWh_p PR - (CAPEX + CP + OPEX + N_T OP)$$

$$B_{\text{fixed}} = \sum_{j=1}^{25} SYkWh_p PR - (CAPEX + OPEX)$$

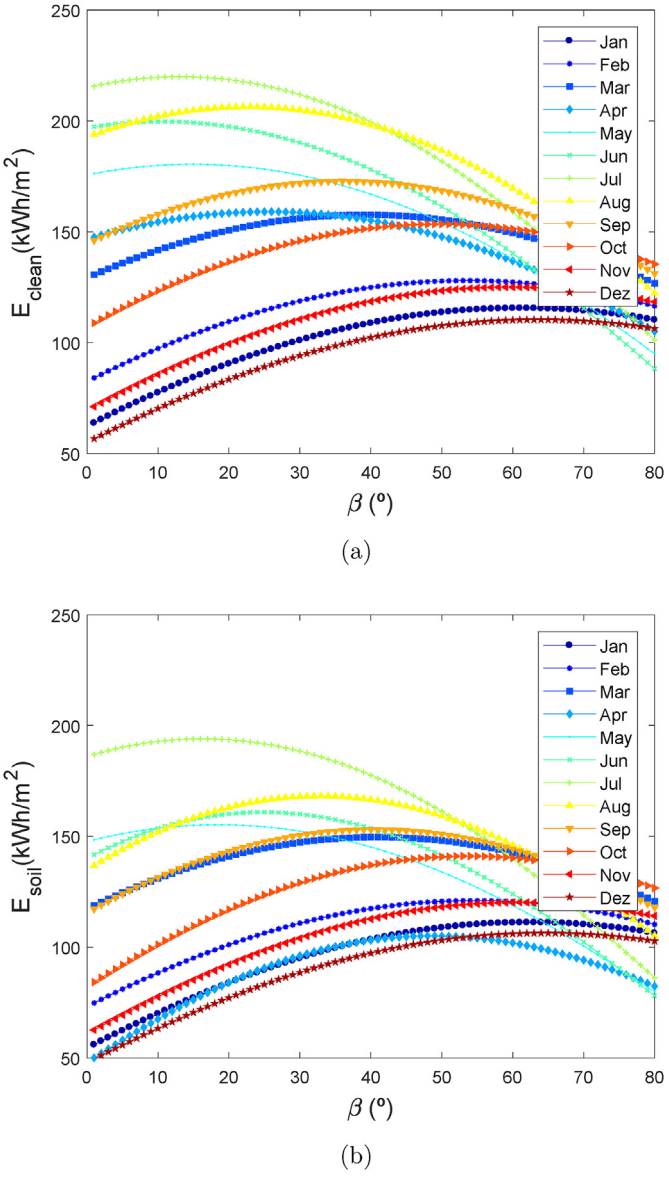

Fig. 6. Effective energy for: (a) clean scenario; (b) soiled scenario.

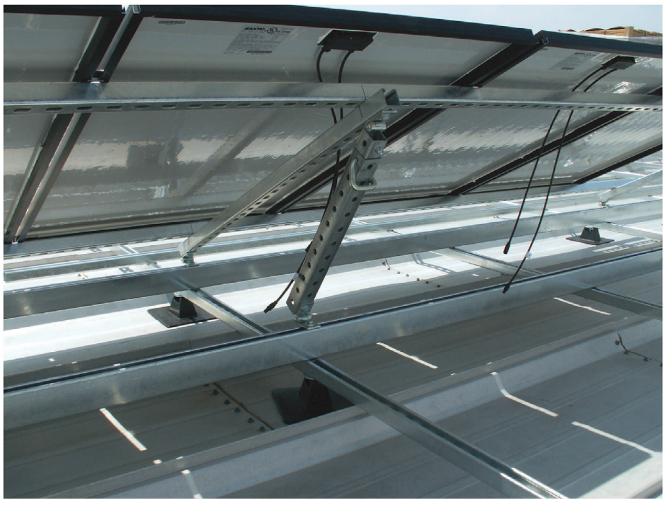

Fig. 7. UNISTRUT Service Company movable PV frame.

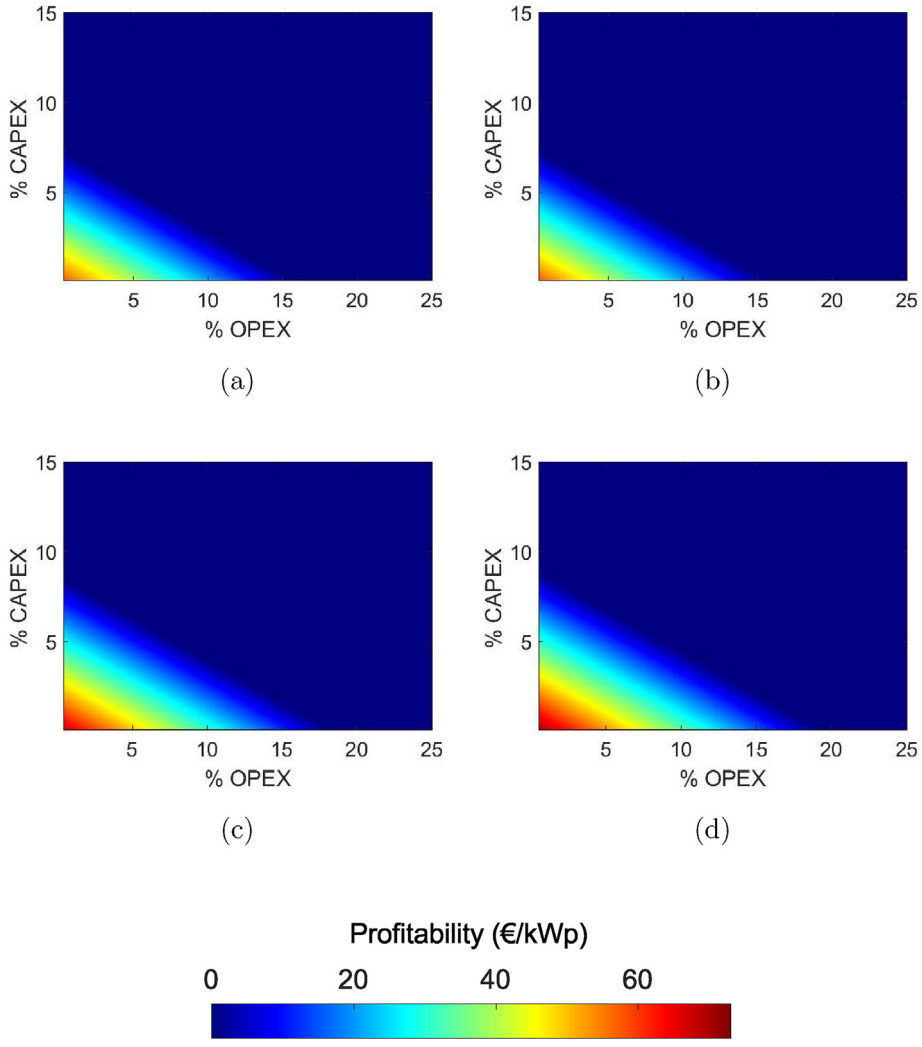

Fig. 8. Profitability index for: (a) 2 tilt angles; (b) 3 tilt angles; (c) 4 tilt angles; (d) 5 tilt angles.

For simplicity reasons, In Fig. 8, a representation of Eq. (15) is only shown for 2, 3, 4 and 5 tilt angles. A triangular area can be observed, denominated profitability area, P_A, which is common for all figures. It should be noted that, all figures, including the ones not presented, depict a profitable area, even for low variation values of *CAPEX* and *OPEX*, such as 0.1%, which may not be a realistic result. Moreover, it can be observed from Fig. 8, that an increase in the number of tilt angles along the year leads to an increase in the *OPEX* and *CAPEX* variation, for which there can be profit. This is expected, since changing tilt angles can increase costs, but at the same time, it is compensated by the increase in the energy production. The area where more profit can be made is the one for which the variation of both *CAPEX* and *OPEX* is close to zero, which may not be realistic. In order to find the optimum configuration, a parameter was created to relate profitability area with the sum of the profitability index of that same area, denominated weighted profitability, P_W, as calculated through Eq. (16):

$$P_W = \frac{\iint_A PI \, dx \, dy}{P_A} \tag{16}$$

In order to evaluate the sensitivity of this index to energy prices, several values were considered, as shown in Fig. 9. According to the chosen criterion, results show that the optimum configuration, is the 4 tilt angle one. Adding more tilt angles throughout the year does not increase substantially the weighted profitability. It should be noted that the optimum configuration is independent of the energy price, except for very low values, which is to be expected, since the gain becomes meaningless. It can also be noticed that the weighted profitability decreases with the energy price reduction, considering that the energy production, relatively to the fixed configuration, is not compensated by low energy prices. Predicted values of *CAPEX* and *OPEX* for 2050 from Ref. [19] are used in Fig. 9b. For the same energy price, the weighted profitability window is larger, mainly because the predicted values of *CAPEX* and *OPEX* will be lower than the ones in 2017.

This analysis shows that in the future, and under the current conditions, it may be even more profitable to have a PV plant with movable frames instead of a fixed installations. Nevertheless, it is stated that this is a simple analysis and therefore, larger data sets should be considered when a more robust economic analysis is taken into account.

4. Cleaning schedule modelling

Many PV system owners may not have the economic capacity to invest in a movable system or either the know-how to design their systems *a priori* considering soiling effect. However, to ensure

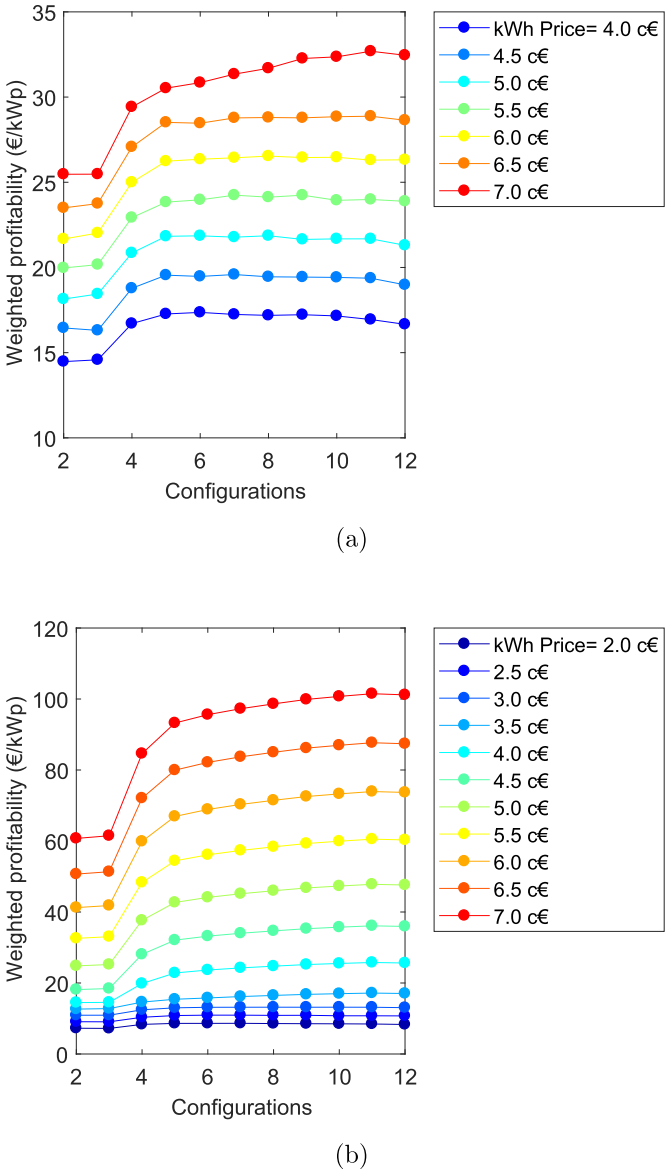

Fig. 9. Profitability window for two cases, including different energy prices: (a) year 2017; (b) year 2050.

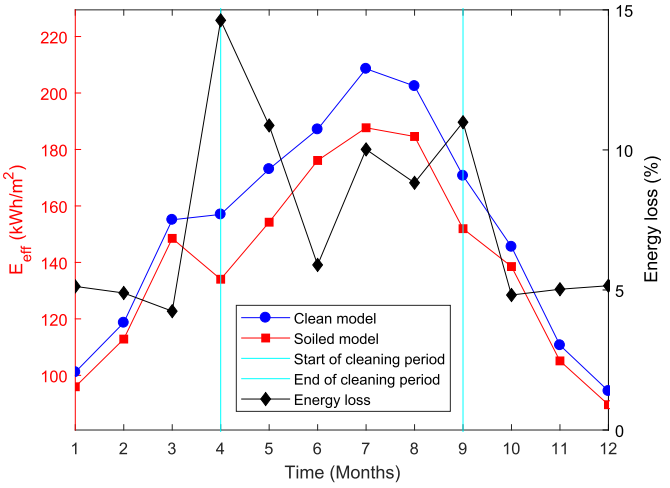

Fig. 10. Cleaning schedule as a function of soiling. Blue dots represent the clean scenario, red squares represent the soiled scenario, light blue vertical lines represent the cleaning period and black diamonds depict the energy loss between the clean and soiled scenarios. (For interpretation of the references to colour in this figure legend, the reader is referred to the Web version of this article.)

maximum efficiency, it is necessary to know the optimum cleaning schedule. In this context, the energy production evolution of both clean and soiled models for the same tilt angle and a specific configuration was determined, as shown in Fig. 10:

When considering the particular case for this location, results for the energy production with constant tilt angle throughout the year, see Fig. 10, demonstrate that if a loss higher than 5% in the energy produced is not desired, a periodic cleaning from April to September should be carried out. Other thresholds can be chosen as desired and respective cleaning periods can be determined.

5. Conclusions

The present work includes a modified effective irradiance model, in the sense that local soiling was used, constants had to be recalculated and its use expanded. This allowed the inclusion of soiling effect in the determination of the tilt angle, optimizing the energy production in comparison to the one solely calculated from irradiance. This approach created the opportunity to calculate the optimum tilt for a static PV system designed to ignore cleaning tasks, while maximizing its energy output. Moreover, the model was also used to calculate multiple optimum tilt angle designs to maximize the annual energy output, which can be performed with simple movable frames and also taking into account that no cleaning is required. For large PV plants, it could be interesting to increase energy production with a quasi-static system using movable tilt angle frames, rather than 2-axis or 1-axis tracking systems, usually associated with higher maintenance costs and higher downtime due to lower reliability. Considering the tilt angle moving costs, energy production and with the consequent economic analysis, the optimum design for a multiple tilt angle configuration along the year was found. The established model was also used as a method to define a cleaning schedule, i.e. the identification of necessary cleaning periods to achieve a desired efficiency range. It should be noted that generalization to other locations is feasible and that larger data sets of soiling are needed in order to increase the model robustness.

Acknowledgments

Ricardo Conceição and F.M. Lopes acknowledge the FCT scholarship SFRH/BD/116344/2016 and SFRH/BD/129580/2017, respectively. All authors are grateful to the Renewable Energies Chair (University of Évora) for supporting this work and to the Water Laboratory, University of Évora, for the use of the spectrophotometer. All authors acknowledge the European Commission's Joint Research Centre, which made the Photovoltaic Geographical Information System (PVGIS). Hugo Silva acknowledges the support from the project DNI-A with the reference ALT20-03-0145-FEDER-000011. This work was co-funded by the European Union through the European Regional Development Fund, framed in COMPETE 2020 (Operational Program Competitiveness and Internationalization) through ICT (UID/GEO/04683/2013) with reference POCI-01-0145-FEDER-007690.

Appendix

Table 3
Optimum tilt angles, effective energy and gain comparison between different configurations for the respective periods. The first column in Table 3 has all the possible combinations of configurations (e.g. 1 angle, 2 angles) with the tilt angles for both soiled and clean scenarios, β_C and β_S, on column two and three, respectively. The fourth and fifth columns correspond to the respective periods for each of the optimum tilt angles in each configuration, for clean and soiled scenarios, respectively. The sixth and seventh columns correspond to the effective energy in each configuration, for both clean and soiled models, respectively. The eighth column corresponds to the effective energy gain for each soiled configuration regarding the soiled fixed one.

Nº tilts	β_C (º)	β_S (º)	MonthC	MonthS	E_{eff}^{C} (kWh/m^2)	E_{eff}^{S}(kWh/m^2)	R_{SS} (%)
1	34	40	1–12	1–12	1843	1617	–
2	51	52	1-3 & 9-12	1-4 & 9-12	1911	1670	3.2
	17	24	4–8	5–8			
3	50	51	1–3	1–4	1912	1671	3.3
	17	26	4–8	5–9			
	51	59	9–12	10–12			
4	50	51	1–3	1–4	1918	1679	3.8
	17	20	4–8	5–7			
	36	36	9	8–9			
	57	59	10–12	10–12			
5	57	58	1–2	1–2	1922	1682	4.0
	39	45	3	3–4			
	17	20	4–8	5–7			
	36	36	9	8–9			
	57	59	10–12	10–12			
6	57	58	1–2	1–2	1926	1683	4.1
	32	45	3–4	3–4			
	13	20	5–7	5–7			
	23	36	8	8–9			
	36	54	9	10			
	57	63	10–12	11–12			
7	57	58	1–2	1–2	1928	1684	4.1
	39	45	3	3–4			
	26	20	4	5–7			
	13	33	5–7	8			
	23	41	8	9			
	36	54	9	10			
	57	63	10–12	11–12			
8	57	58	1–2	1–2	1928	1685	4.2
	39	45	3	3–4			
	26	22	4	5–6			
	13	16	5–7	7			
	23	33	8	8			
	36	41	9	9			
	50	54	10	10			
	62	63	11–12	11–12			
9	61	58	1	1–2	1928	1685	4.2
	54	41	2	3			
	39	49	3	4			
	26	22	4	5–6			
	13	16	5–7	7			
	23	33	8	8			
	36	41	9	9			
	50	54	10	10			
	62	63	11–12	11–12			
10	61	58	1	1–2	1928	1686	4.2
	54	41	2	3			
	39	49	3	4			
	26	18	4	5			
	15	25	5	6			
	12	16	6–7	7			
	23	33	8	8			
	36	41	9	9			
	50	54	10	10			
	62	63	11–12	11–12			
11	61	62	1	1	1928	1686	4.3
	54	55	2	2			
	39	41	3	3			
	26	49	4	4			
	15	18	5	5			
	12	25	6–7	6			
	23	16	8	7			
	36	33	9	8			
	50	41	10	9			
	60	54	11	10			
	64	63	12	11–12			
12	61	62	1	1	1929	1687	4.3
	54	55	2	2			
	39	41	3	3			

(*continued on next page*)

Table 3 (*continued*)

Nº tilts	β_C (º)	β_S (º)	MonthC	MonthS	E_{eff}^{C} (kWh/m^2)	E_{eff}^{S}(kWh/m^2)	R_{SS} (%)
	26	49	4	4			
	15	18	5	5			
	10	25	6	6			
	13	16	7	7			
	23	33	8	8			
	36	41	9	9			
	50	54	10	10			
	60	61	11	11			
	64	65	12	12			

References

[1] C. Perpiña, C. Batista, S. Lavalle, An assessment of the regional potential for solar power generation in EU-28, Energy Pol. 88 (2016) 86–99.

[2] M.R. Maghami, H. Hizam, C. Gomes, M.A. Radzi, M.I. Rezadad, S. Hajighorbani, Power loss due to soiling on solar panel, Renew. Sustain. Energy Rev. 59 (2016) 1307–1316.

[3] S.A. Kalogirou, R. Agathokleous, G. Panayiotou, On-site PV characterization and the effect of soiling on their performance, Energy 51 (2013) 439–446.

[4] J. Mallineni, K. Yedidi, S. Shrestha, B. Knisely, S. Tatapudi, J. Kuitche, G. Tamizhmani, Soiling losses of utility-scale PV systems in hot-dry desert climates: results from four 4-16 years old power plants, in: 2014 IEEE 40th Photovolt. Spec. Conf. PVSC 2014, 2014, pp. 3197–3200.

[5] R. Conceição, H. Silva, J. Mirão, M. Gostein, L. Fialho, L. Narvarte, M. Collares-Pereira, Saharan dust transport to Europe and its impact on photovoltaic performance: a case study of soiling in Portugal, Sol. Energy 160 (2018) 94–102.

[6] R. Conceição, H.G. Silva, M. Collares-Pereira, CSP mirror soiling characterization and modeling, Sol. Energy Mater. Sol. Cells 185 (March) (2018) 233–239.

[7] A.A. Hegazy, Effect of dust accumulation on solar transmittance through glass covers of plate-type collectors, Renew. Energy 22 (2001) 525–540.

[8] B. Mondoc, F. Pop, Factors influencing the performance of a photovoltaic power plant, in: 3rd Int. Conf. Mod. Power Syst. MPS 2010, 2010, pp. 18–21.

[9] P.D. Burton, B.H. King, Artificial soiling of photovoltaic module surfaces using traceable soil components, Conf. Rec. IEEE Photovolt. Spec. Conf. (2013) 1542–1545.

[10] R. Xu, K. Ni, Y. Hu, J. Si, H. Wen, D. Yu, Analysis of the optimum tilt angle for a soiled PV panel, Energy Convers. Manag. 148 (2017) 100–109.

[11] J. Lu, S. Hajimirza, Optimizing sun-tracking angle for higher irradiance collection of PV panels using a particle-based dust accumulation model with gravity effect, Sol. Energy 158 (April) (2017) 71–82.

[12] C.A. Gueymard, From global horizontal to global tilted irradiance: how accurate are solar energy engineering predictions in practice?, in: Solar Conference, San Diego, CA, Am. Sol. Energy, 2008.

[13] B.Y. Liu, R.C. Jordan, The interrelationship and characteristic distribution of direct, diffuse and total solar radiation, Sol. Energy 4 (3) (1960) 1–19.

[14] M. Collares-Pereira, A. Rabl, The average distribution of solar radiation-correlations between diffuse and hemispherical and between daily and hourly insolation values, Sol. Energy 22 (2) (1979) 155–164.

[15] T. Huld, R. Müller, A. Gambardella, A new solar radiation database for estimating PV performance in Europe and Africa, Sol. Energy 86 (6) (2012) 1803–1815.

[16] N. Martin, J.M. Ruiz, Calculation of the PV modules angular losses under field conditions by means of an analytical model, Sol. Energy Mater. Sol. Cells 70 (2001) 25–38.

[17] R. Conceição, H. Silva, J. Mirão, M. Collares-Pereira, Organic soiling: the role of pollen in PV module performance degradation, Energies (2018) 1–13.

[18] M. García, L. Marroyo, E. Lorenzo, M. Pérez, Soiling and other optical losses in solar-tracking PV plants in navarra, Prog. Photovoltaics Res. Appl. 19 (2) (2011) 211–217.

[19] C.B. Eero Vartiainen, Gaëtan Masson, The True Competitiveness of Solar PV: a European Case Study, Tech. rep., European PV Technology and Innovation Platform Steering Comittee PV LCOE and Competitiveness Working Group, 2017.